

See discussions, stats, and author profiles for this publication at: <https://www.researchgate.net/publication/23443503>

# Preparation and Characterization of Simple Dihalomethylidene Platinum Dihalide Complexes in Reactions of Laser-Ablated Pt Atoms with Tetrahalomethanes

ARTICLE in JOURNAL OF THE AMERICAN CHEMICAL SOCIETY · DECEMBER 2008

Impact Factor: 12.11 · DOI: 10.1021/ja805862j · Source: PubMed

---

CITATIONS

30

---

READS

14

2 AUTHORS, INCLUDING:



Han-Gook Cho

Incheon National University

81 PUBLICATIONS 1,392 CITATIONS

SEE PROFILE

# Preparation and Characterization of Simple Dihalomethylidene Platinum Dihalide Complexes in Reactions of Laser-Ablated Pt Atoms with Tetrahalomethanes

Han-Gook Cho and Lester Andrews\*

Department of Chemistry, University of Incheon, 177 Dohwa-dong, Nam-ku, Incheon, 402-749, South Korea, and Department of Chemistry, University of Virginia, P.O. Box 400319, Charlottesville, Virginia 22904-4319

Received July 26, 2008; E-mail: lsa@virginia.edu

**Abstract:** Platinum atoms react with tetrachlorofluoromethanes upon laser-ablation and with ultraviolet irradiation to form dihalomethylidene platinum dihalide complexes,  $CX_2=PtX_2$ . These new molecules are identified from carbon-13 and chlorine isotopic shifts, displacements in functional group frequencies as chlorine is replaced with fluorine, and comparison to frequencies calculated by density functional theory. The Pt–C bond lengths calculated here, 1.810 to 1.816 Å, are shorter than analogous bond lengths measured earlier for Pt(II) carbene complexes (1.943–1.950 Å). The computed effective Pt–C bond orders range from 1.41 to 1.70 as chlorine is replaced by fluorine since the more electronegative halogen appears to concentrate the Pt 5d orbitals and make them bond better with carbon. These platinum methylidene complexes thus have a substantial amount of double bond character from  $d_\pi$ – $p_\pi$  bonding.

## Introduction

A large number of platinum carbene complexes have been prepared, and their role as reagents or intermediates in catalytic and C–H activation reactions was investigated.<sup>1</sup> For example cyclopropyl platinum carbenes have been proposed as reactive intermediates in cyclo-isomerization reactions.<sup>2,3</sup> Additional relevant cases include aminocarbene and dihalobis(alcoxyalkylidene)complexes of platinum(II). X-ray structures of the former complexes have found 1.943–1.950 Å Pt–C bond lengths that are shortened due to partial  $d_\pi$ – $p_\pi$  bonding as further established by DFT calculations.<sup>4</sup> Reactions of diazomethane derivatives provide a source of platinum carbene intermediates, which give rise to species with slightly shortened Pt–C bonds.<sup>5</sup> Fischer-carbene platinum complexes are formed by reactions of alkynes and alcohols with platinum salts. These bis(alcoxyalkylidene) complexes contain similar 1.932–1.956 Å Pt–C bond lengths.<sup>6</sup> Although platinum(II) complexes have been studied extensively, fewer platinum(IV) complexes have been prepared, and these include such examples as dicyclopentadienyl bis, cationic, and

hydrido(alkyl) carbenes.<sup>7</sup> We are aware of no examples of smaller platinum methylidene complexes.

A new generation of simple methylidene complexes has been prepared by reactions of laser-ablated transition metal atoms and methane or halomethanes.<sup>8</sup> The reactions proceed through C–H(X) insertion followed by  $\alpha$ -H(X) transfer. With favorable reaction energetics, methylidyne complexes are often formed depending on the stability of higher metal oxidation states. These reactions appear to be more favorable with tetrahalomethanes than with methane itself.<sup>8,9</sup> Accordingly we applied this approach to platinum to prepare simple platinum methylidene complexes through oxidative addition reactions with tetrahalomethanes. Here we report matrix infrared spectra and density functional theory calculations of simple dihalomethylidene platinum dihalide complexes, which contain platinum–carbon bonds with substantial  $\pi$ -bonding character.

## Experimental and Computational Methods

Laser-ablated platinum atoms were reacted with  $CF_4$ ,  $CF_3Cl$ ,  $CF_2Cl_2$ ,  $CFCl_3$  (Du Pont),  $CCl_4$  (Fisher),  $^{13}CCl_4$  (90% enriched, MSD Isotopes),  $CF_3Br$ , and  $CF_2ClBr$  (PCR Research) in excess argon during condensation at 10 K using a closed-cycle refrigerator (Air Products Displex). These methods have been described in detail

- (1) (a) Herndon, J. W. *Coord. Chem. Rev.* **2008**, 252, in press. (b) Herndon, J. W. *Coord. Chem. Rev.* **2007**, 251, 1158. (c) Herndon, J. W. *Coord. Chem. Rev.* **2006**, 250, 1889. (d) Herndon, J. W. *Coord. Chem. Rev.* **2005**, 249, 999. (e) Herndon, J. W. *Coord. Chem. Rev.* **2004**, 248, 3 and earlier review articles in this series.
- (2) Aubert, C.; Buisine, O.; Malacria, M. *Chem. Rev.* **2002**, 102, 813 and references therein.
- (3) Mamane, V.; Grees, T.; Krause, H.; Furstner, A. *J. Am. Chem. Soc.* **2004**, 126, 8655.
- (4) Gosavi, T.; Wagner, C.; Merzweiler, K.; Schmidt, H.; Steinborn, D. *Organometallics* **2005**, 24, 533.
- (5) (a) Hanks, T. W.; Ekeland, R. A.; Emerson, K.; Larsen, R. D.; Jennings, P. W. *Organometallics* **1987**, 6, 28. (b) Poverenov, E.; Leitens, G.; Shinon, L. J. W.; Milstein, D. *Organometallics* **2005**, 24, 5937.
- (6) Werner, M.; Lis, T.; Bruhn, C.; Lindar, R.; Steinborn, K. *Organometallics* **2006**, 25, 5946.

- (7) (a) Zhang, S.-W.; Takahashi, S. *Organometallics* **1998**, 17, 4757, and references therein. (b) Rendina, L. M.; Vittal, J. J.; Puddephatt, R. J. *Organometallics* **1995**, 14, 1030. (c) Prokopchuk, E. M.; Puddephatt, R. J. *Organometallics* **2003**, 22, 563, and references therein. (d) Zhang, F.; Prokopchuk, E. M.; Broczkowski, M. E.; Jennings, M. C.; Puddephatt, R. J. *Organometallics* **2006**, 25, 1583, and references therein.
- (8) Andrews, L.; Cho, H.-G. *Organometallics* **2006**, 25, 4040, and references therein (Review article).
- (9) Lyon, J. T.; Cho, H.-G.; Andrews, L. *Organometallics* **2007**, 26, 6373 (Cr, Mo, W +  $CHX_3$ ,  $CX_4$ ).

in previous publications.<sup>8–10</sup> Reagent gas mixtures ranged 0.5–1.0% in argon. The Nd:YAG laser fundamental (1064 nm, 10 Hz repetition rate, 10 ns pulse width) was focused on a rotating platinum metal target (crucible piece, American Platinum Works) using 5–20 mJ/pulse. After initial reaction, infrared spectra were recorded at a resolution of 0.5 cm<sup>-1</sup> using a Nicolet 550 spectrometer with a Hg–Cd–Te range B detector (low frequency limit 420 cm<sup>-1</sup>). Samples were later irradiated for 20 min periods by a mercury arc street lamp (175 W) with the globe removed using a combination of optical filters and subsequently annealed to allow further reagent diffusion.

To provide support for the assignment of new experimental frequencies and to correlate with related works,<sup>8,9</sup> density functional theory (DFT) calculations were performed using the Gaussian 03 program system,<sup>11</sup> the B3LYP density functional,<sup>12</sup> the 6-311++G(3df,3pd) basis sets for C, F, Cl, Br,<sup>13</sup> and the SDD pseudopotential and basis set<sup>14</sup> for Pt to provide vibrational frequencies for the reaction products. Geometries were fully relaxed during optimization, and the optimized geometry was confirmed by vibrational analysis. The BPW91<sup>15</sup> functional was also employed to complement the B3LYP results. Natural bond orbital (NBO) analysis<sup>11,16</sup> was done to help understand the bonding. The vibrational frequencies were calculated analytically, and zero-point energy is included in the calculation of binding and reaction energies. Previous investigations have shown that DFT calculated harmonic frequencies are usually slightly higher than observed frequencies,<sup>8–10,17,18</sup> and they provide useful predictions for infrared spectra of new molecules.

## Results and Discussion

Reactions of platinum with tetrahalomethane precursor molecules were investigated, and infrared spectra and density functional frequency calculations of the products will be presented in turn.

**CCl<sub>4</sub>.** The reaction of laser-ablated Pt atoms with carbon tetrachloride in excess argon during condensation at 8 K produced two strong new absorptions at 1008.3 cm<sup>-1</sup> (1003.1 cm<sup>-1</sup> satellite for matrix site splitting) and 886.5 cm<sup>-1</sup> (884.6 cm<sup>-1</sup> shoulder for chlorine isotopic splitting) (labeled **m** for methylidene) along with bands at 1036.4 cm<sup>-1</sup> (CCl<sub>3</sub><sup>+</sup>), 1019.3 and 926.7 cm<sup>-1</sup> (Cl<sub>2</sub>CCl–Cl), and 898 cm<sup>-1</sup> (CCl<sub>3</sub>), which are illustrated in Figure 1a. The latter bands are common to all laser-ablated metal experiments with CCl<sub>4</sub> through photolysis by the ablation plume, and their identification follows from earlier formation using vacuum ultraviolet irradiation.<sup>19–22</sup> The new

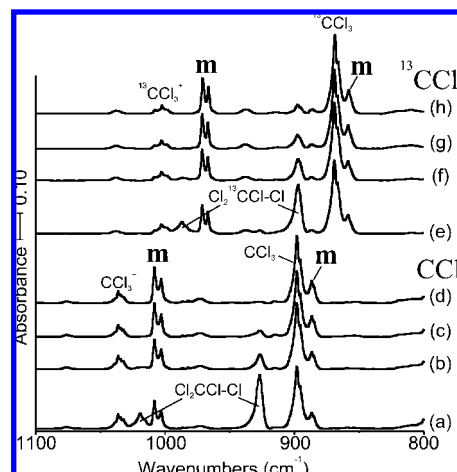


**Figure 1.** Infrared spectra in the 1100–800 cm<sup>-1</sup> region for the laser-ablated platinum atom and carbon tetrachloride reaction products in excess argon at 10 K. (a) Pt and CCl<sub>4</sub> (0.5% in argon) codeposited for 1 h, (b) after visible ( $\lambda > 420$  nm) irradiation for 20 min, (c) after ultraviolet (240–380 nm) irradiation for 20 min, and (d) after full arc ( $\lambda > 220$  nm) irradiation for 20 min. (e) Pt and <sup>13</sup>CCl<sub>4</sub> (0.5% in argon, 90% enriched) codeposited for 1 h, (f) after visible ( $\lambda > 420$  nm) irradiation for 20 min, (g) after ultraviolet (240–380 nm) irradiation for 20 min, and (h) after full arc ( $\lambda > 220$  nm) irradiation for 20 min.

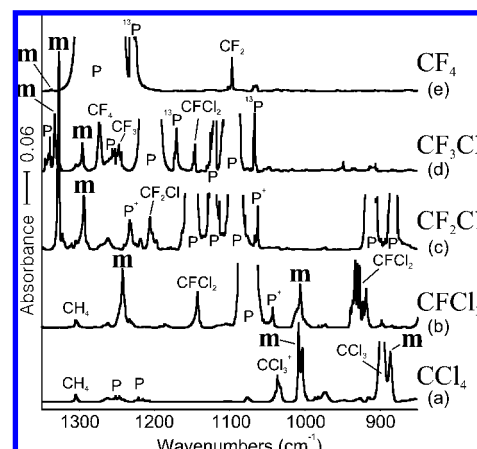


**Figure 2.** Infrared spectra in the 1350–850 cm<sup>-1</sup> region for the laser-ablated platinum atom and tetrafluorochloromethane reaction products in excess argon at 10 K. Illustrated spectra recorded after Pt and reagent (0.5% in argon) codeposited for 1 h and subjected to mercury arc irradiation sequence described in Figure 1 caption. (a) CCl<sub>4</sub>, (b) CFCl<sub>3</sub>, (c) CF<sub>2</sub>Cl<sub>2</sub>, (d) CF<sub>3</sub>Cl, and (e) CF<sub>4</sub>.

absorptions increased in concert 10, 20, and 5% on irradiations in the visible ( $\lambda > 420$  nm), ultraviolet (240–380 nm), and full arc ( $\lambda > 220$  nm) regions, respectively. Annealing to 28 K sharpened the bands and resolved the 884.6 cm<sup>-1</sup> shoulder. A similar experiment with <sup>13</sup>CCl<sub>4</sub> (90% enriched) shifted the new absorptions to 971.4 cm<sup>-1</sup> (966.9 cm<sup>-1</sup> satellite) and to 858.5 cm<sup>-1</sup> (856.1 cm<sup>-1</sup> shoulder). The appearance of the <sup>12</sup>C product bands with approximately one-tenth of the <sup>13</sup>C product band absorbance confirms that a single carbon atom participates in these vibrational modes.

**Chlorofluoromethanes.** Infrared spectra from the reaction of Pt atoms with chlorofluoromethanes are compared in Figure 2 with the spectrum for carbon tetrachloride and for carbon

- (10) (a) Andrews, L.; Citra, A. *Chem. Rev.* **2002**, 102, 885, and references therein. (b) Andrews, L. *Chem. Soc. Rev.* **2004**, 33, 123, and references therein.
- (11) Kudin, K. N.; et al. *Gaussian 03*, revision B.04, Gaussian, Inc.: Pittsburgh, PA, 2003.
- (12) (a) Becke, A. D. *J. Chem. Phys.* **1993**, 98, 5648. (b) Lee, C.; Yang, Y.; Parr, R. G. *Phys. Rev. B* **1988**, 37, 785.
- (13) Raghavachari, K.; Trucks, G. W. *J. Chem. Phys.* **1989**, 91, 1062.
- (14) Andrae, D.; Haeussermann, U.; Dolg, M.; Stoll, H.; Preuss, H. *Theor. Chim. Acta* **1990**, 77, 123.
- (15) (a) Becke, A. D. *Phys. Rev. A* **1988**, 38, 3098. (b) Burke, K.; Perdew, J. P.; Wang, Y. In *Electronic Density Functional Theory: Recent Progress and New Directions*; Dobson, J. F., Vignale, G., Das, M. P., Ed.; Plenum: 1998.
- (16) (a) Reed, A. E.; Weinhold, F. *J. Chem. Phys.* **1985**, 83, 735. (b) Reed, A. E.; Curtiss, L. A.; Weinhold, F. *Chem. Rev.* **1988**, 88, 899.
- (17) Scott, A. P.; Radom, L. *J. Phys. Chem.* **1996**, 100, 16502.
- (18) Andersson, M. P.; Uvdal, P. L. *J. Phys. Chem. A* **2005**, 109, 3937.
- (19) Andrews, L. *J. Chem. Phys.* **1968**, 48, 972.
- (20) (a) Jacox, M. E.; Milligan, D. E. *J. Chem. Phys.* **1971**, 54, 3935. (b) See also: Jacox, M. E. *J. Phys. Chem. Ref. Data* **1994**, Monograph 3; **1998**, 27 (2), 115 and references therein.
- (21) Prochaska, F. T.; Andrews, L. *J. Chem. Phys.* **1977**, 67, 1091, and references therein.

- (22) Maier, G.; Reisenauer, H. P.; Hu, J.; Hess, B. A., Jr.; Schaad, L. J. *Tetrahedron Lett.* **1989**, 30, 4105.

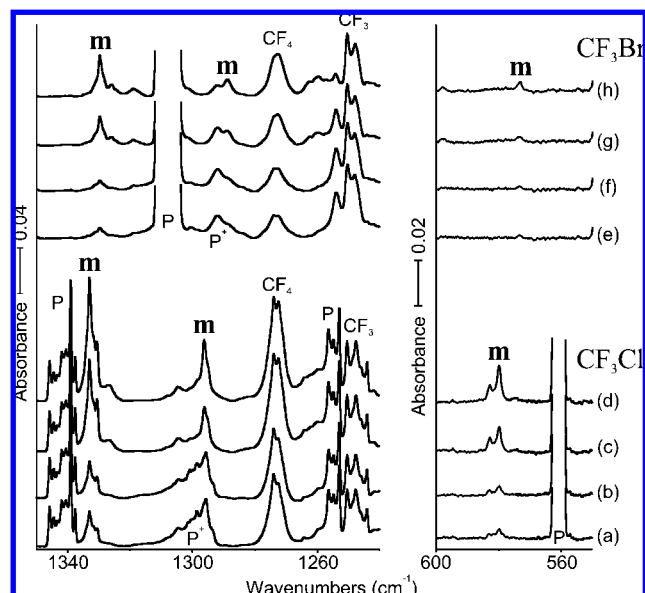


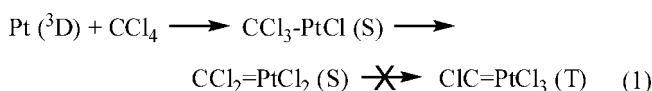
**Figure 3.** Infrared spectra in the 1350–1240 and 600–550  $\text{cm}^{-1}$  regions for the laser-ablated platinum atom and trifluorohalomethane reaction products in excess argon at 10 K. (a) Pt and  $\text{CF}_3\text{Cl}$  (0.5% in argon) codeposited for 1 h, (b) after visible ( $\lambda > 420$  nm) irradiation for 20 min, (c) after ultraviolet (240–380 nm) irradiation for 20 min, and (d) after full arc ( $\lambda > 220$  nm) irradiation for 20 min. (e) Pt and  $\text{CF}_3\text{Br}$  (0.5% in argon) codeposited for 1 h, (f) after visible ( $\lambda > 420$  nm) irradiation for 20 min, (g) after ultraviolet (240–380 nm) irradiation for 20 min, and (h) after full arc ( $\lambda > 220$  nm) irradiation for 20 min.

tetrafluoride all shown after full arc irradiation ( $> 220$  nm). This irradiation maximizes the new product band absorbance (labeled **m** for each reaction), as displayed in Figure 1 for the  $\text{CCl}_4$  reaction product. Precursor bands (labeled P) block out large portions of the spectrum, but this cannot be avoided. Absorptions from precursor cation or daughter radical products formed by exposure to ultraviolet radiation from the Pt target emission plume are labeled accordingly, as taken from earlier works.<sup>19–24</sup> Two new bands were observed for  $\text{CFCl}_3$ , one at  $1242.7\text{ cm}^{-1}$  in the C–F stretching region, and one at  $1006.2\text{ cm}^{-1}$  near the strongest absorption for the  $\text{CCl}_4$  product. These bands increased in concert 10% on visible, 100% on ultraviolet, and 10% on full arc irradiation (not shown). Reaction with the  $\text{CF}_2\text{Cl}_2$  precursor gave two strong bands at  $1327.3$  and  $1293.9\text{ cm}^{-1}$  in the C–F stretching region and a weaker band at  $730.1\text{ cm}^{-1}$  in the  $\text{CF}_2$  bending region (not shown), which were not changed on visible, increased 125% on ultraviolet, and increased 20% on full arc irradiation to reach the strongest product absorptions observed here. The  $\text{CF}_3\text{Cl}$  reaction revealed similar strong bands at  $1333.0$  and  $1296.2\text{ cm}^{-1}$ . More detailed spectra in Figure 3 show that the  $1296.2\text{ cm}^{-1}$  band appears first as a shoulder on the side of the parent cation byproduct in the C–F stretching region, and a weaker new band is also found at  $579.8\text{ cm}^{-1}$ . These bands increase in concert a factor of 4 during the irradiation sequence. Notice that the parent cation absorption at  $1295.2\text{ cm}^{-1}$  decreases on full arc irradiation<sup>23</sup> while the new **m** product band at  $1296.2\text{ cm}^{-1}$  increases. Finally, the  $\text{CF}_4$  reaction revealed one weak band at  $1336.8\text{ cm}^{-1}$  (absorbance

0.002) illustrated at the top left of Figure 2, which increased by 50% on ultraviolet irradiation.

**Bromofluoromethanes.** Infrared spectra recorded after reaction of Pt with two related bromine derivatives followed the same patterns. The  $\text{CF}_2\text{ClBr}$  precursor gave strong  $1324.9$ ,  $1320.4\text{ cm}^{-1}$  and weaker  $1270.2$ ,  $1262.5\text{ cm}^{-1}$  bands split by the matrix interaction (not shown). The  $\text{CF}_3\text{Br}$  reaction with Pt revealed almost identical bands to  $\text{CF}_3\text{Cl}$ , now shifted to  $1329.3$  and  $1288.8\text{ cm}^{-1}$  in the C–F stretching region, and a similar band at  $573.3\text{ cm}^{-1}$ , which are also shown in Figure 3. Notice that the new **m** product band is now better resolved from the  $1292.0\text{ cm}^{-1}$  parent cation band.<sup>24</sup> Although the overall product yield was lower, these three bands also increased together in intensity a factor of 4 under the series of mercury arc irradiations.

**Calculations.** A large body of work in our laboratory has shown that laser-ablated transition metal atoms react with halomethanes through C–X bond activation/insertion followed by  $\alpha$ -X transfer to give lower energy products,<sup>8,9</sup> reaction 1.



The singlet insertion product is 64 kcal/mol lower in energy than the reagents, but the singlet methyldene is 87 kcal/mol lower (i.e., reaction 1 is exothermic, (S) indicates singlet electronic state, and (T) denotes triplet). A triplet methyldene is 29 kcal/mol higher than the singlet, so we believe that the singlet methyldene is the global minimum energy product. In this case the second  $\alpha$ -Cl transfer would give a 50 kcal/mol higher energy triplet or 58 kcal/mol higher energy singlet  $\text{ClC-PtCl}_3$  product, for which we have no experimental evidence. Energies for the methyldene formation reaction as a function of fluorine substitution in the precursor were calculated, and surprisingly these become much less exothermic with fluorine substitution for chlorine. The values are  $\text{CCl}_2\text{=PtCl}_2$  (–87 kcal/mol),  $\text{CFCl=PtCl}_2$  (–81),  $\text{CCl}_2\text{=PtFCl}$  (–61),  $\text{CF}_2\text{=PtCl}_2$  (–76),  $\text{CFCl=PtFCl}$  (–54),  $\text{CCl}_2\text{=PtF}_2$  (–34),  $\text{CF}_2\text{=PtFCl}$  (–48),  $\text{CFCl=PtF}_2$  (–26), and  $\text{CF}_2\text{=PtF}_2$  (–20). In this regard, the bromine substituted methyldene  $\text{CFBr=PtF}_2$  is 28 kcal/mol higher energy than the isomer  $\text{CF}_2\text{=PtFBr}$ . The reactions of Mo and W atoms with  $\text{CCl}_4$  are also more exothermic than their  $\text{CF}_4$  counterparts,<sup>9</sup> but not by the relative magnitude found here for Pt.

Frequency and structure calculations were performed for each methyldene product; the frequencies are listed in Tables 1, 2, and S1, for five molecules, and the structures are compared in Figure 4. The BPW91 functional gives lower product frequencies than the B3LYP functional, as expected,<sup>17,18</sup> but in this case the frequencies are much lower and clearly do not fit as well with experimental values as the B3LYP data (Table 1). NBO analysis was performed for each platinum methyldene complex, and insightful bonding parameters are compared in Table 3.

**$\text{CCl}_2\text{=PtCl}_2$ .** The two strong  $1008.3$  and  $886.5\text{ cm}^{-1}$  product absorptions from the reaction of Pt and  $\text{CCl}_4$  in solid argon are assigned to the  $\text{CCl}_2\text{=PtCl}_2$  methyldene for the following reasons. First, the observed bands are 1% and 2% higher than the harmonic frequencies calculated for the two strongest modes of this minimum energy product using the B3LYP density functional. Although observed frequencies are usually slightly lower than the DFT calculated values,<sup>17,18</sup> this is not always the case for heavy metal halides, as shown by our recent

(23) (a) Prochaska, F. T.; Andrews, L. *J. Chem. Phys.* **1978**, 68, 5568, and references therein. (b) Prochaska, F. T.; Andrews, L. *J. Chem. Phys.* **1978**, 68, 5577, and references therein.

(24) Prochaska, F. T.; Andrews, L. *J. Phys. Chem.* **1978**, 82, 1731, and references therein.



**Table 1.** Observed and Calculated Fundamental Frequencies of the  $\text{CCl}_2=\text{PtCl}_2$  Methylidene in the Ground  $^1\text{A}_1$  Electronic State with the  $\text{C}_{2v}$  Structure<sup>a</sup>

approximate description	$^{12}\text{CCl}_2=\text{PtCl}_2$					$^{13}\text{CCl}_2=\text{PtCl}_2$				
	obsd	B3LYP	int	BPW91	int	obsd	B3LYP	int	BPW91	int
$\text{Cl}_2=\text{C}=\text{Pt}$ str, $b_1$	1008.3	999.9	284	981.5	242	971.4	963.3	264	945.4	225
$\text{C}-\text{Cl}$ str, $b_2$	886.5	869.7	198	838.9	190	858.5	841.6	185	811.8	178
$\text{CCl}_2$ wag, $b_1$		451.1	0	427.9	5		434.7	0	427.5	5
$\text{CCl}_2$ bend, $c_1$		438.9	4	426.6	0		438.5	3	411.4	0
$\text{Pt}-\text{Cl}$ str, $b_1$		365.3	69	367.9	60		365.1	68	367.5	60
$\text{Pt}-\text{Cl}$ str, $a_1$		349.1	8	350.9	8		349.1	8	350.9	8
$\text{CCl}_2$ def, $a_1$		227.7	0	222.0	0		227.7	0	222.0	0
$\text{CCl}_2$ rock, $b_2$		213.2	0	207.2	0		212.3	0	206.4	0
$\text{PtCl}_2$ wag, $b_2$		102.2 <sup>d</sup>	1	101.4	1		102.2	1	101.4	1

<sup>a</sup>Frequencies and intensities are in  $\text{cm}^{-1}$  and  $\text{km/mol}$ . Observed in an argon matrix. Frequencies and intensities computed with B3LYP/6-311++G(3df,3pd) in the harmonic approximation using the SDD core potential and basis set for Pt and using the BPW91 functional. Symmetry notations are based on the  $\text{C}_{2v}$  structure. <sup>b</sup>Mode has antisymmetric  $\text{Cl}_2=\text{C}=\text{Pt}$  stretching character. <sup>c</sup>Mode has some symmetric  $\text{Cl}_2=\text{C}=\text{Pt}$  stretching character. <sup>d</sup>Three real 96, 65, and  $23\text{ cm}^{-1}$  frequencies are not listed.

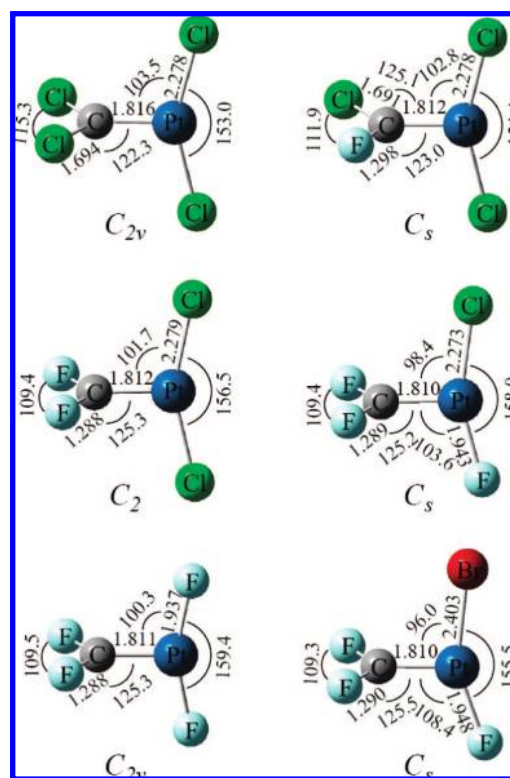
**Table 2.** Observed and Calculated Fundamental Frequencies of the  $\text{CF}_2=\text{PtFCl}$  and  $\text{CF}_2=\text{PtFBr}$  Methylidenes in Ground  $^1\text{A}'$  Electronic States with Essentially  $\text{C}_s$  Structures<sup>a</sup>

approximate description	$\text{CF}_2=\text{PtFCl}$			$\text{CF}_2=\text{PtFBr}$		
	obsd	calcd	int	obsd	calcd	int
$\text{F}-\text{C}=\text{Pt}$ str, $b_1$	1333.0	1336.4	654	1329.3	1332.8	633
$\text{C}-\text{F}$ str, $a''$	1296.2	1275.3	198	1288.8	1269.9	215
$\text{CF}_2$ bend, $a'$		731.0	4		730.4	4
$\text{Pt}-\text{F}$ str, $a'$	579.8	590.6	114	573.3	583.7	131
$\text{C}-\text{F}_2$ wag, $a'$		577.6	6		564.5	0
$\text{CF}_2$ bend, $c_1$		383.4	4		382.9	8
$\text{Pt}-\text{Cl}, \text{Br}$ str, $a'$		366.3	19		250.8	7
$\text{CF}_2$ rock, $a''$		325.7	0		324.3	0
$\text{F}-\text{Pt}-\text{Cl}, \text{Br}$ def, $a''$		150.7	4		141.6	3

<sup>a</sup>Frequencies and intensities are in  $\text{cm}^{-1}$  and  $\text{km/mol}$ . Observed in an argon matrix. Frequencies and intensities computed with B3LYP/6-311++G(3df,3pd) in the harmonic approximation using the SDD core potential and basis set for Pt. Symmetry notations are based on the  $\text{C}_s$  structure. Three real 131, 75, and  $24\text{ cm}^{-1}$  frequencies are not listed. <sup>b</sup>Mode has some antisymmetric  $\text{F}_2=\text{C}=\text{Pt}$  stretching character. <sup>c</sup>Mode has some symmetric  $\text{F}_2=\text{C}=\text{Pt}$  stretching character.

investigations.<sup>9</sup> Thus, the close agreement between calculated and observed frequencies (Table 1) is reassuring. The same frequency pattern is found with the BPW91 functional, but the values are lower still, as typically observed.<sup>17,18</sup> In addition, the strongest calculated (B3LYP) absorption for the 23 kcal/mol higher energy  $\text{CCl}_3-\text{PtCl}$  insertion product at  $838\text{ cm}^{-1}$  is not detected. Second, the carbon-13 shifts, 36.9 and  $28.0\text{ cm}^{-1}$ , observed for the two strong bands very nearly match the computed values, 36.6 and  $28.1\text{ cm}^{-1}$ , as the observed 12/13 isotopic frequency ratios 1.037 99 and 1.032 62 are almost the same as the calculated frequency ratios, 1.037 99 and 1.033 39. This means that the calculation is describing the same normal modes as observed for the reaction product, and it reinforces the match in the calculated frequency position and high intensities. Third, the  $886.5\text{ cm}^{-1}$  product band and  $884.6\text{ cm}^{-1}$  shoulder have the appropriate 9/6 relative intensity for natural abundance chlorine isotopes (35,35/35,37 statistical population) for a vibration involving two equivalent chlorine atoms. The calculation predicts a  $2.0\text{ cm}^{-1}$  shift, and we observe a  $1.9\text{ cm}^{-1}$  shift for this isotopic effect.

Interestingly, the  $1008.3\text{ cm}^{-1}$  vibrational coordinate involves mostly  $\text{Pt}=\text{C}$  stretching mixed with symmetric  $\text{C}-\text{Cl}_2$  displacement. For a pure symmetric  $\text{Cl}-\text{C}-\text{Cl}$  stretching mode with the  $115.3^\circ$  valence angle calculated here, the 12/13 isotopic frequency ratio would be 1.025 03, which is substantially less than the observed 1.03799 value. This underscores the description of this normal mode as C vibrating back and forth between

**Figure 4.** Structures calculated for the tetrahaloplatinum methylidene complexes at the B3LYP level of theory using the 6-311++G(3df,3pd) basis sets for C, F, Cl, Br and SDD pseudopotential and basis set for Pt. Bond distances, Å, and angles, deg. Molecular symmetries are given under each structure.

Pt and two Cl atoms. The calculated  $438.9\text{ cm}^{-1}$  mode with only a  $0.4\text{ cm}^{-1}$  carbon-13 shift is the symmetric  $\text{Cl}_2=\text{C}=\text{Pt}$  stretching counterpart, which involves little carbon motion. Our best prediction of a  $\text{Pt}=\text{C}$  stretching frequency for these molecules comes from B3LYP calculations for  $\text{CH}_2=\text{PtH}_2$ , which has a similar ( $1.790\text{ Å}$ )  $\text{Pt}=\text{C}$  bond length. The computed  $868\text{ cm}^{-1}$  mode for  $\text{CH}_2=\text{PtH}_2$  has 77% of the C-13 shift for a pure diatomic  $\text{Pt}=\text{C}$  stretching mode and a deuterium shift of  $112\text{ cm}^{-1}$ , so even this mostly  $\text{Pt}=\text{C}$  stretching mode is mixed with a H bending motion.

**$\text{CFCl}=\text{PtCl}_2$ .** The  $\text{CFCl}_3$  reaction gives almost as strong product bands as  $\text{CCl}_4$ , one in the  $\text{C}-\text{F}$  stretching region at  $1242.7\text{ cm}^{-1}$  and one at  $1006.2\text{ cm}^{-1}$ , near the strongest band for  $\text{CCl}_2=\text{PtCl}_2$  (Figure 2). The lowest energy product for this

**Table 3.** Parameters from Natural Bond Order Analysis for  $\text{CX}_2=\text{PtX}_2$  Methylidene Complexes and Ethylene<sup>a</sup>

orbital occup.	% C <sup>b</sup>	% Pt <sup>c</sup>	Orb. occ.	% C <sup>b</sup>	% Pt <sup>c</sup>
<b>CCl<sub>2</sub>=PtCl<sub>2</sub></b>					
$\sigma(1.92)$	59.4	40.6	$\sigma(1.61)$	26.1	73.9
	37% s, 63% p	42% s, 58% d	$\pi(1.95)$	60.6	39.4
$\pi(1.58)$	38.4	61.6	$\sigma^*(0.35)$	73.9	26.1
	100% p	31% p, 69% d	$\pi^*(0.17)$	39.4	60.6
$\sigma^*(0.22)$	40.6	59.4	<b>1.52</b>		
	37% s, 63% p	42% s, 58% d			
$\pi^*(0.47)$	61.6	38.4	<b>CF<sub>2</sub>=PtFCl</b>		
<b>1.41</b>	100% p	31% p, 69% d	$\sigma(1.88)$	24.0	76.0
			$\pi(1.93)$	56.1	43.9
<b>CCl<sub>2</sub>=PtFCl</b>					
$\sigma(1.92)$	59.6	40.4	$\sigma^*(0.38)$	76.0	24.0
$\pi(1.59)$	32.2	67.8	$\pi^*(0.23)$	43.9	56.1
$\sigma^*(0.20)$	40.4	59.6	<b>1.60</b>		
$\pi^*(0.40)$	67.8	32.2			
<b>1.46</b>			<b>CF<sub>2</sub>=PtF<sub>2</sub></b>		
			$\sigma(1.95)$	61.8	38.2
<b>CCl<sub>2</sub>=PtF<sub>2</sub></b>					
$\sigma(1.93)$	60.5	39.5	$\pi(1.95)$	20.4	79.6
$\pi(1.94)$	26.3	72.7	$\sigma^*(0.13)$	30.2	61.8
$\sigma^*(0.17)$	39.5	60.5	$\pi^*(0.35)$	79.6	20.4
$\pi^*(0.48)$	72.7	27.3	<b>1.71</b>		
<b>1.61</b>			<b>CH<sub>2</sub>=CH<sub>2</sub></b>		
			$\sigma(1.995)$	50.0, 50.0	
			$\pi(1.999)$	50.0, 50.0	
			$\sigma^*(0.003)$	50.0, 50.0	
			$\pi^*(0.000)$	50.0, 50.0	
			<b>1.995</b>		

<sup>a</sup> Computed with B3LYP/6-311++G(3df, 3pd). SDD core potential and basis set are used for Pt. Resulting Effective Bond Order given in bold type. <sup>b</sup> Percent carbon in the orbital at left: carbon valence orbitals given below. <sup>c</sup> Percent platinum in the orbital at left: platinum valence orbitals given below.

stoichiometry,  $\text{CFCl}=\text{PtCl}_2$ , has the strongest calculated frequencies at  $1252.3\text{ cm}^{-1}$  (356 km/mol) and  $993.5\text{ cm}^{-1}$  (331 km/mol) (Table S1), which have a similar relationship as the two  $\text{CCl}_2=\text{PtCl}_2$  bands. The C–F mode is calculated 0.8% high, and again the C–Cl mode low, this time by 1.3%. The fact that no Pt–F stretching mode is observed rules out the 20 kcal/mol higher energy structural isomer  $\text{CCl}_2=\text{PtFCl}$  complex. The  $1006.2\text{ cm}^{-1}$  band is due to the antisymmetric motion of C between FCl and Pt, namely the antisymmetric  $\text{FCl}-\text{C}=\text{Pt}$  stretching mode, analogous to the  $1008.3\text{ cm}^{-1}$  absorption for the  $\text{CCl}_2=\text{PtCl}_2$  methylidene.

**$\text{CF}_2=\text{PtCl}_2$  and  $\text{CF}_2=\text{PtClBr}$ .** The strongest bands were observed for the  $\text{CF}_2\text{Cl}_2$  reaction, and these are diagnostic: two C–F stretching modes and one  $\text{CF}_2$  bending mode at  $1327.3$ ,  $1293.9$ , and  $730.1\text{ cm}^{-1}$ . These bands are in excellent agreement with the three highest calculated frequencies for the  $\text{CF}_2=\text{PtCl}_2$  methylidene, namely,  $1333.1\text{ cm}^{-1}$  (684 km/mol),  $1276.5\text{ cm}^{-1}$  (216 km/mol), and  $730.8\text{ cm}^{-1}$  (5 km/mol), for these modes as described (Table S1). Note the very high intensity for the highest frequency band, which involves carbon vibrating between Pt and two F atoms. Hence, this mode also exhibits some  $\text{Pt}=\text{C}$  stretching character, but less so than the  $1008.3\text{ cm}^{-1}$  band for the  $\text{CCl}_2=\text{PtCl}_2$  methylidene. There is no evidence for a diagnostic C–Cl stretching mode near  $1000\text{ cm}^{-1}$  like that observed for the first two reaction products.

The  $\text{CF}_2\text{ClBr}$  reaction produced strong  $1324.9$ ,  $1320.4\text{ cm}^{-1}$  and weaker  $1270.2$ ,  $1262.5\text{ cm}^{-1}$  bands split by the matrix and just below those for  $\text{CF}_2\text{Cl}_2$ . The B3LYP calculation predicted strong  $\text{CF}_2$  stretching modes at  $1329.8\text{ cm}^{-1}$  (692 km/mol) and  $1271.6\text{ cm}^{-1}$  (212 km/mol) for  $\text{CF}_2=\text{PtClBr}$ , which substantiates this assignment.

**$\text{CF}_2=\text{PtFCl}$  and  $\text{CF}_2=\text{PtFBr}$ .** The  $\text{CF}_3\text{Cl}$  reaction product again exhibits two strong C–F stretching modes, now slightly higher at  $1333.0$  and  $1296.2\text{ cm}^{-1}$ , and a Pt–F stretching mode at  $579.8\text{ cm}^{-1}$ . The stable platinum fluoride is  $\text{PtF}_6$ , and this strong antisymmetric stretching mode is higher at  $695\text{ cm}^{-1}$ .<sup>25</sup> The calculated and observed frequencies are compared in Table 2 with those at  $1329.3$ ,  $1288.8$ , and  $573.3\text{ cm}^{-1}$  from the analogous  $\text{CF}_3\text{Br}$  reaction. Again, the computed frequencies correlate closely with the observed values: the calculated symmetric modes are 0.3% higher and the antisymmetric modes are 1.5% lower than the observed values. The strongest band at  $1333.0\text{ cm}^{-1}$  is the symmetric C–F<sub>2</sub> stretching mode coupled with the  $\text{C}=\text{Pt}$  stretching motion, based on calculated displacement coordinates, and the weaker  $1296.2\text{ cm}^{-1}$  band is the antisymmetric C–F stretching mode. The  $579.8\text{ cm}^{-1}$  band is due to the Pt–F stretching mode as described by computed displacement coordinates.

Now, compare the calculated and observed effects of Br substitution for Cl. For reference, the very strong antisymmetric C–F stretching modes of  $\text{CF}_3\text{Cl}$  and  $\text{CF}_3\text{Br}$  appear at  $1205$  and  $1198\text{ cm}^{-1}$  in solid argon, and the symmetric counterparts absorb at  $1097$  and  $1076\text{ cm}^{-1}$ , respectively. Notice the small heavy halogen shifts for the product,  $3.7\text{ cm}^{-1}$  for the symmetric  $\text{CF}_2$  stretch and  $7.4\text{ cm}^{-1}$  for the antisymmetric  $\text{CF}_2$  stretch, roughly 30–50% of that found for the precursor molecules where the heavy halogen is bonded to the carbon supporting the C–F vibrations under consideration. These small shifts in C–F stretching modes in the product demonstrate that the heavy halogen is removed from the carbon center, as the product structures indicate, and the heavy Pt atom mechanically dampens the effect. Not so for the Pt–F stretching mode, which shifts  $6.5\text{ cm}^{-1}$  (from  $579.8$  to  $573.3\text{ cm}^{-1}$ ) when the adjacent Pt–Cl is replaced by Pt–Br. Our calculations predict  $6.9\text{ cm}^{-1}$  for this shift in Pt–F modes and  $3.6$  and  $5.4\text{ cm}^{-1}$  displacements for the two C–F modes, which represents very good agreement between the observed and computed frequencies for  $\text{CF}_2=\text{PtFCl}$  and  $\text{CF}_2=\text{PtFBr}$ .

**$\text{CF}_2=\text{PtF}_2$ .** One very weak band was observed for the  $\text{CF}_4$  reaction at  $1336.8\text{ cm}^{-1}$ , which corresponds to the strongest mode computed for the  $\text{CF}_2=\text{PtF}_2$  product at  $1341.8\text{ cm}^{-1}$  (610 km/mol). The antisymmetric mode calculated at  $1278.9\text{ cm}^{-1}$  (225 km/mol) is covered by the strong precursor absorption. We were not able to detect the stronger Pt–F stretching mode computed at  $615.3\text{ cm}^{-1}$  (156 km/mol). Although the one band we observe for this species is weak, the correlation with the calculated strongest C–F stretching modes is compelling. The above assignments cover the range of observed values  $3$ – $10\text{ cm}^{-1}$  lower than calculated values, and the  $5\text{ cm}^{-1}$  difference for  $\text{CF}_2=\text{PtF}_2$  is in agreement. The yield of the perfluoro methylidene product is much lower than that of the perchloro product because energetics favor reaction 1 substantially over the  $\text{CF}_4$  analogue. Also, the much larger and more polarizable electron cloud for  $\text{CCl}_4$  probably undergoes faster oxidative addition reactions with metal atoms than the smaller, more compact  $\text{CF}_4$  molecule. In our experience both C–Cl activation and  $\alpha$ -Cl transfer are more favorable than the corresponding processes with fluorine.<sup>8,9</sup> Finally, notice that the symmetric C–F<sub>2</sub> stretching mode increases from  $1327.3$  to  $1333.0$  to  $1336.8\text{ cm}^{-1}$  in the series  $\text{CF}_2=\text{PtCl}_2$ ,  $\text{CF}_2=\text{PtFCl}$ ,  $\text{CF}_2=\text{PtF}_2$  and the antisymmetric C–F<sub>2</sub> counterpart increases from  $1293.9$

(25) Holloway, J. H.; Stanger, G.; Hope, E. G.; Levason, W.; Ogden, J. S. *J. Chem. Soc., Dalton Trans.* **1988**, 1341.

to 1296.2 cm<sup>-1</sup> for the first two members of this series as the heavier chlorine is replaced by the lighter fluorine substituent on platinum.

To summarize, the excellent agreement between observed spectra and one to three of the strongest calculated frequencies for the above related seven CX<sub>2</sub>=PtX<sub>2</sub> molecules confirms our preparation of these platinum methylidene complexes.

**Structures.** The structures for six methylidene complexes are illustrated in Figure 4. The structures have one or two planes of symmetry except for CF<sub>2</sub>=PtCl<sub>2</sub>, which has none (the computed F—C—Pt—Cl dihedral angle is 96.0°). Next, notice that the C=Pt bond length decreases from 1.816 Å for CCl<sub>2</sub>=PtCl<sub>2</sub> to 1.810 Å for CF<sub>2</sub>=PtFCl with increasing fluorine substitution. This is in contrast to the group 4 and Th metal ClC÷MCl<sub>3</sub> and FC÷MF<sub>3</sub> complexes [the divide symbol represents a triplet state carbene complex] where fluorine substitution increases the carbon—metal bond length by 0.02 to 0.05 Å and the group 6 methylidyne where the triple bond lengths are essentially the same.<sup>9,26,27</sup>

Another comparison can be made of the subject Pt—Cl bond lengths computed here between 2.273 and 2.279 Å and those measured for a cationic Pt(IV) carbene complex at 2.378 and 2.289 Å<sup>7b</sup> and Pt(II) carbene complexes in the 2.367 to 2.377 Å range.<sup>4,6</sup> To provide a simple basis for comparison, we calculated the PtCl<sub>2</sub> and PtCl<sub>4</sub> molecules using the B3LYP method and find triplet ground states with 2.189 and 2.270 Å bond lengths, respectively. We suggest that our computed 2.276(4) Å Pt—Cl complex bond length is a consequence of the effectively higher oxidation state of Pt in our difluoro- and dichloromethylidene platinumdichloride complexes.

**Bonding.** Natural bond orbital analysis computations were performed to gain insight into the platinum—carbon bond, and these parameters are listed in Table 3. The Pt—C orbitals and their occupancies are given. The effective bond order (EBO) is bonding minus antibonding occupancies divided by two, and these values (listed in bold type in the table) range from 1.41 to 1.71. Clearly there is substantial  $\pi$  bonding and double bond character in our platinum methylidene complexes, although not a full double bond as comparison with CH<sub>2</sub>=CH<sub>2</sub> itself shows. Notice the regular increase in EBO with fluorine substitution for chlorine. Apparently the more electronegative F contracts the platinum 5d orbitals and makes them more compatible for bonding to carbon 2p orbitals. This point is substantiated by comparing the EBO for CCl<sub>2</sub>=PtCl<sub>2</sub> (1.41), the two symmetrical difluorodichloro-substituted CF<sub>2</sub>=PtCl<sub>2</sub> (1.52) and CCl<sub>2</sub>=PtF<sub>2</sub> (1.61) methylidenes, and CF<sub>2</sub>=PtF<sub>2</sub> (1.71). There is more increase in EBO in the difluoroplatinum case than with difluorocarbon substitution. The carbon and platinum percent contributions to each orbital are also given. There is some

variation with fluorine substitution in both bonding and anti-bonding orbitals as the inductive effect of the fluorine is felt by the valence orbitals of the host atom.

Further comparisons to larger organometallic platinum carbene complexes are of interest. Puddephatt et al. found a Pt=C distance of 1.99(2) Å and a Pt—CH<sub>3</sub> distance of 2.13(2) Å in a cationic Pt(IV) complex,<sup>7b</sup> and Steinborn and co-workers compared the Pt—C bond lengths measured (1.943–1.950 Å) for their Pt(II) amino carbene complex with the median Pt—C single bond length (2.04 Å) and suggested that the shorter bond exhibits partial d $\pi$ —p $\pi$  bonding.<sup>4</sup> DFT calculations support this conclusion and find comparable bond lengths to those measured. Our DFT computed Pt—C bond lengths in the 1.810 to 1.816 Å range clearly indicate substantially more localized platinum—carbon d $\pi$ —p $\pi$  bonding although not a full double bond based on the computed EBO values including ethylene itself (Table 3). It is reasonable to conclude that we have a higher effective oxidation state for Pt in these new methylidene complexes than in typical Pt(II) carbenes and that our platinum dihalide methylidene complexes appear to have substantial Pt(IV) character.

## Conclusions

Laser-ablated Pt atoms react with tetrahalomethanes to form dihalomethylidene platinum dihalide complexes, CX<sub>2</sub>=PtX<sub>2</sub>. The identification is based on carbon-13 and chlorine isotopic shifts, displacements in functional group frequencies as chlorine is replaced with fluorine or bromine, and comparison to frequencies calculated by density functional theory. The reaction is substantially more exothermic and the yield much higher for X = Cl than X = F. The computed effective Pt—C bond orders range from 1.41 to 1.70 as chlorine is replaced by fluorine, since the more electronegative halogen appears to concentrate the Pt 5d orbitals and to make them bond more strongly with carbon. The CX<sub>2</sub>=PtX<sub>2</sub> methylidene complexes thus have a substantial amount of double bond character from d $\pi$ —p $\pi$  bonding. The Pt—C bond lengths calculated here, 1.810 to 1.816 Å, are shorter than bond lengths measured for Pt(IV) (1.99(2) Å)<sup>7b</sup> and Pt(II) carbene complexes (1.943–1.950 Å).<sup>4,6</sup> In spite of the extensive literature for Pt(II) carbene complexes,<sup>1–6</sup> we believe that this is the first investigation of simple platinum methylidene complexes and that our platinum dihalide methylidene complexes have substantial Pt(IV) character.

**Acknowledgment.** We gratefully acknowledge financial support from the National Science Foundation (U.S.) Grant CHE 03-52487 to L.A. and support from the Korea Institute of Science and Technology Information (KISTI) by Grant No. KSC-2008-S02-0001.

**Supporting Information Available:** Complete ref 11. Table S1 comparing observed and calculated frequencies. This material is available free of charge via the Internet at <http://pubs.acs.org>.

JA805862J

(26) Lyon, J. T.; Cho, H.-G.; Andrews, L. *Organometallics* **2007**, 26, 2519 (Ti, Zr, Hf + CHX<sub>3</sub>, CX<sub>4</sub>).

(27) Lyon, J. T.; Cho, H.-G.; Andrews, L. *Eur. J. Inorg. Chem.* **2008**, 1047 (Th + CHX<sub>3</sub>, CX<sub>4</sub>).